Frustration effects on the electronic density of states of a random binary alloy

Gerardo G. Naumis,[1] Chumin Wang,[2] and Rafael A. Barrio[1]
[1]*Instituto de Física, Universidad Nacional Autónoma de México (UNAM), Apartado Postal 20-364, 01000, México D.F., Mexico*
[2]*Instituto de Investigaciones en Materiales, UNAM, Apartado Postal 70-360, 04510, México D.F., Mexico*
(Received 15 March 2001; revised manuscript received 6 December 2001; published 19 March 2002)

We examine the tight-binding density of states of a random binary alloy in a square lattice. In the split-band limit, which is similar to the model used for studing the quantum percolation problem, numerical calculations show that there is a pseudogap at the center of the lower subband, near and beyond the geometrical percolation threshold. This behavior is studied in two ways, by analyzing the first spectral moments of the lower subband, and by taking advantage of the bipartite nature of the lattice to renormalize half of the sites. This shows that the pseudogap in the split band limit appears because of frustration effects in the renormalized lattice.

DOI: 10.1103/PhysRevB.65.134203 PACS number(s): 71.23.An, 73.20.At

I. INTRODUCTION

It is well known that when a metallic system is perturbed by adding impurities, its simple electronic band is modified. Tails of localized states appear at the edges of the band and there are two mobility edges that separate extended and localized states. If disorder is strong enough, there is an Anderson transition when the two mobility edges merge.[1] These ideas can be studied with great precision in a random binary alloy using computer simulations in large two- and three-dimensional lattices, where disorder is generally introduced within a nearest-neighbor tight-binding scheme. For example, Kirkpatrick and Eggarter (KE)[2] investigated numerically a random binary alloy of 1500 sites and found that in the split band limit, many degenerate localized states appear exactly at the center of the lower subband, and a pseudogap starts building up around these localized states. The number of these states at the center and depth of the pseudogap increases as the concentration of atoms with larger site energy increases. Furthermore, this pseudogap appears before the concentration of forbidden sites (with infinite site energies) percolate through the system. While numerical work by KE has been very useful to show failure of the coherent potential approximation (CPA) in the split band limit,[3] not much theoretical work has been done to explain their interesting results.

Recently, this problem has been given renewed interest, since it shares many features with the quantum percolation problem in the split-band limit. In this work we will focus our attention on the pseudogap that appears in the density of states, which certainly has a direct impact on the optical and other physical properties of the alloy and will not address the fascinating problem of metallic conductivity. The study of the bands in the random binary alloy may be relevant to the quantum percolation problem, since in the split-band limit, geometrical percolation has an impact not only on the band structure but also on the different degrees of localization of electronic states. It is worthwhile mentioning that there remains a controversy obviously in literature about the spectral structure and the localization properties in the quantum percolation problem. In Refs. 4–6 the transfer matrix formalism was used, and the results seem to agree with the scaling approach[7] in the sense that all states are localized in two-dimensional systems even above the percolation threshold. However, Meir *et al.*[8] found a localization transition for finite concentration near the percolation threshold. Later, it was argued that the results of Meir *et al.* were inexact[9] and that there is no transition in the type of localization.

The spectrum of the vertex problem in a quasiperiodic Penrose lattice also shares many features with the random binary alloy.[10–12] In fact, in the Penrose lattice there are confined states[13,14] that appear precisely at the center of the band, separated from the rest of the states by a gap.[13,15] The existence of gaps in quasiperiodic lattices is important, since it has been suggested that a pseudogap caused by a Hume-Rothery mechanism leads to the stabilization of quasicrystals,[16,17] as it does for binary alloys.[18]

In this paper, we concentrate on a disordered two-dimensional square lattice and show that the existence of a pseudogap at the center of the spectrum in the random binary alloy can be addressed by studying the frustration of the wave function in a renormalized sublattice, which is obtained from the bipartite property of the lattice. A lattice is bipartite if it can be subdivided into two alternating sublattices, say, α and β, and an electron can only hop from an α site onto a β site or back. The Hamiltonian can then be renormalized in such a way that the center of the spectrum is mapped into a band edge.[15] The common features between the Penrose tiling and the binary alloy are due to the bipartite character of the lattices. To analyze the opening of a pseudogap, we start by calculating the first spectral moments of the spectrum, using the Cyrot-Lackmann theorem,[19] which relates the local density of states (LDOS) to the topology of the local atomic environment.

The structure of this paper is as follows. In Sec. II the model is described and some numerical results in large lattices are shown. Then, the first spectral moments of the binary alloy are evaluated, using the Cyrot-Lackmann theorem. The tendency for a pseudogap to form is obtained by examining the normalized fourth moment. In Sec. III, we show that the bipartite character allows a renormalization of the Hamiltonian, which leads to the appearance of frustration at the center of the lower subband. Finally, in Sec. IV we conclude with some discussion about the relevant features of this model.

II. PROPERTIES OF THE MODEL

Consider an alloy A_xB_{1-x}, in which the two types of atoms A and B are distributed randomly on a square lattice, with concentrations x and $1-x$, respectively. Within the single-band tight-binding approximation, the Hamiltonian with diagonal disorder can be written as

$$H=\sum |i\rangle \epsilon_i \langle i| + \sum_{\langle i,j\rangle} |i\rangle V \langle j|, \tag{1}$$

where $|i\rangle$ is the orbital at site i, V is a constant hopping integral between nearest-neighbor sites, and the diagonal elements are $\epsilon_i=0(\delta)$ on $A(B)$ sites.

When $\delta \gg ZV$, where $Z=4$ is the coordination number, the spectrum of Eq. (1) splits into two subbands, one centered at $E=0$ and the other at $E=\delta$. This is the so-called split-band limit. The states in the subband around zero energy, which we call the A subband, are strongly confined on A atoms. Furthermore, in the limit $\delta \to \infty$ it has been shown[2] that the B atoms can be formally removed from the problem and that the A subband can be studied by using a Hamiltonian restricted to A sites only

$$H_{AA}=\sum_{i,j\in A} |i\rangle V \langle j|. \tag{2}$$

This Hamiltonian describes an electron that can hop from one site to its neighbors only if both atoms are of type A. Thus, the problem for the A subband is similar to a square-lattice percolation problem, because B atoms act as perfect barriers in the limit of infinite self-energy. However, this problem differs from the geometrical percolation, since the quantum wave function could lose its coherency, even beyond the percolation threshold (which is $x_c^{(s)}=0.59$ for the site problem and $x_c^{(b)}=0.50$ for the bond problem in the square lattice). This lack of coherency is partly due to the frustration of the wave function, as discussed in the next section.

We have verified the results given by KE for larger lattices. Figure 1(a) shows the A subband for $x=0.65$, obtained from an average of 10 randomly chosen configurations of a 3969-site square lattice with periodic boundary conditions and $V=1$. Three main features are visible in the DOS: (1) The spectrum is practically symmetric around $E=0$, since $\delta=1000$ V, (2) there is a pseudogap around the center of the spectrum, and (3) there are many degenerate states at the center. These latter states are strictly confined, even if they can exist in nonisolated clusters.[2] It is worth mentioning that configurations with true gaps and nongaps are always statistically present. Therefore, in a strict sense only a pseudogap should be observed, due to statistical fluctuations. The pseudogap deepens as one approaches the percolation limit, as shown clearly in Fig. 1(b) for $x=0.60$.

The tendency for a pseudogap to open and the symmetry around $E=0$ can be obtained from an analysis of the spectral moments. We start by defining the LDOS at site i as $\rho_i(E)$, then the nth moment is[20,21]

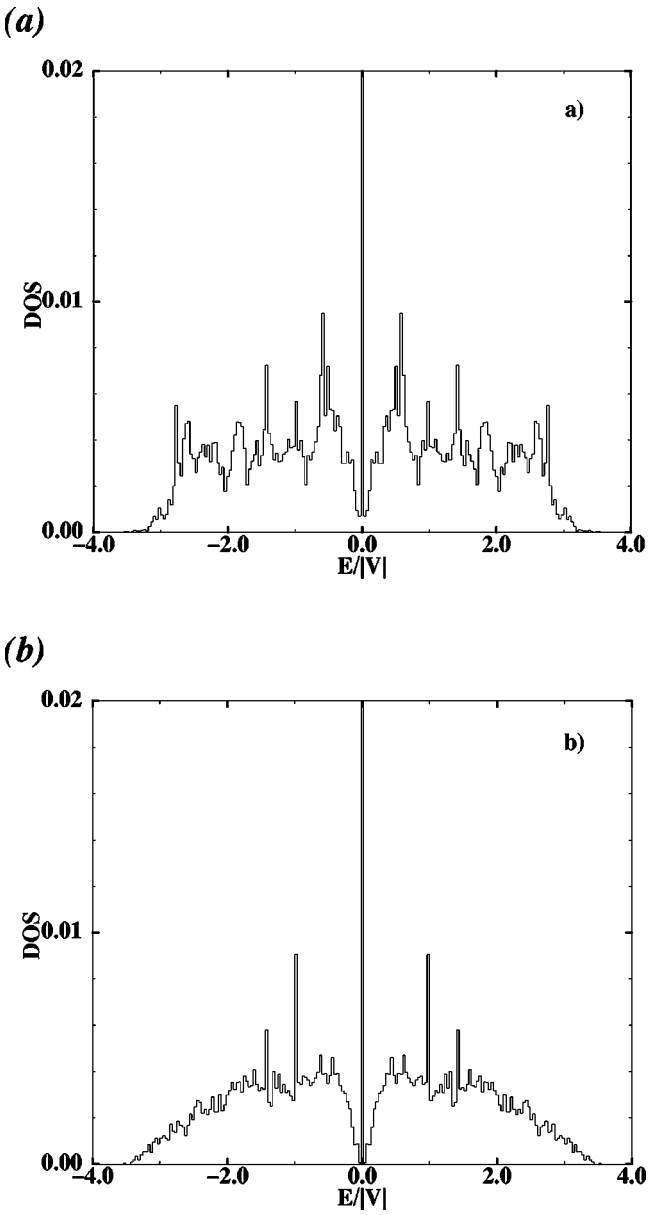

FIG. 1. Average density of states in the A sub-band calculated for ten lattices with 3969 sites. $V=1$, and (a) $x=0.65$, (b) $x=0.60$.

$$\mu_i^{(n)} \equiv \int_{-\infty}^{\infty} (E-H_{ii})^n \rho_i(E) dE = \langle i|(H-H_{ii})^n|i\rangle. \tag{3}$$

The last equality is known as the Cyrot-Lackmann theorem,[19] from which one can obtain the nth moment by counting all possible closed paths with n steps, starting at site i. In the split-band limit we can consider the Hamiltonian (2), and site i should be occupied by an A atom.

The moment $\mu_i^{(0)}$ is always unity, because of the normalization condition of the basis ($\langle i|i\rangle=1$). The first moment $\mu_i^{(1)}$ is the center of gravity of the LDOS, which is $E=0$ in this case ($H_{ii}=0$). The next moment $\mu_i^{(2)}$ is a measure of the ''moment of inertia'' of the LDOS with respect to the center of gravity. The third moment $\mu_i^{(3)}$ measures the skewness

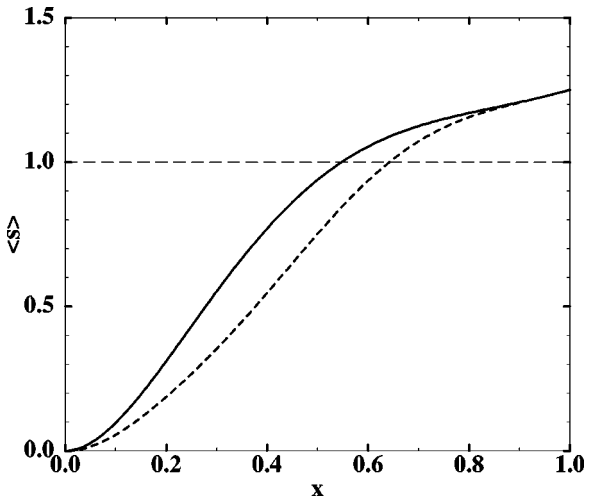

FIG. 2. Parameter $\langle s \rangle$ as a function of the concentration of A atoms. The full line corresponds to Eq. (A13), the critical concentration is at $x=0.55$. The dashed line is the calculation without considering the δ states at $E=0$. Observe that in this case the critical concentration is higher ($x=0.64$).

about the center of gravity. The fourth moment measures the tendency for a *pseudogap* to form at the middle of the spectrum. A useful criterion to discern this tendency is the dimensionless parameter s_i, defined as,[20]

$$s_i = \frac{\mu_i^{(4)}\mu_i^{(2)} - (\mu_i^{(2)})^3 - (\mu_i^{(3)})^2}{(\mu_i^{(2)})^3}. \tag{4}$$

If $s \geqslant 1$ the LDOS is unimodal, while for $s<1$ it is bimodal, which corresponds to two separated peaks in the LDOS.[20] For example, the LDOS of a square lattice is unimodal with a van Hove singularity at $E=0$ and $s=1.25$. A honeycomb lattice has a vanishing LDOS at $E=0$, and $s=0.67$.

In Appendix A, the first four moments of the random binary alloy are calculated in an analytical way, by considering the statistical distribution of paths. In Fig. 2, the full line shows the averaged $\langle s \rangle$ over all sites as a function of x, obtained from Eq. (A13). Notice that $\langle s \rangle < 1$ for $x<0.55$. This number is very close to the geometrical site percolation threshold.

Here, it is important to notice that the confined states at $E=0$ always give a contribution to the unimodal appearance of the LDOS. In order to examine the behavior of band states more exactly, we should exclude the δ states at the center. If the fraction of states at $E=0$ is $f_0(x)$, the band states follow a renormalized LDOS $[\rho_i^*(E)]$, related to the complete LDOS by $\rho_i^*(E)=\lambda(x)\rho_i(E)$, where $\lambda(x)=[1-f_0(x)]^{-1}$, due to the normalization condition.

The moments of $\rho_i^*(E)$ should be scaled in the same fashion, that is, $\mu_i^{*(n)}=\lambda(x)\mu_i^{(n)}$. The corresponding parameter s^* of $\rho_i^*(E)$ is given by

$$s^* = \frac{s+1}{\lambda(x)} - 1 = s[1-f_0(x)] + f_0(x). \tag{5}$$

The quantity $f_0(x)$ is a function of the concentration, and can be taken from KE, who used a local counting in finite clusters, excluding the contribution due to isolated A atoms ($Z=0$). In Fig. 2 we show the scaled version $\langle s^* \rangle$ as a dashed line. The critical concentration is now $x=0.64$, which is well beyond the site percolation threshold ($x_c^{(s)}=0.59$). This fact is consistent with the computational results of KE and us, where a deep pseudogap in the center of the subband appears even for concentrations higher than $x_c^{(s)}$. We point out that $s=1$ does not necessarily coincide with the exact percolation limit, since it is only a measure of the mean value of $\rho(E^2)$ in comparison with its average half width. In the next section, the pseudogap will be analyzed using frustration arguments in a renormalized Hamiltonian.

III. THE SQUARED HAMILTONIAN

A. Definition

The introduction of B atoms produces a tendency for the spectrum to become bimodal. In order to study this, it is convenient to focus on the renormalized Hamiltonian H_{AA}, which takes advantage of the bipartite nature of the A lattice once the B atoms are removed. The bipartite character of the A lattice means that it can be separated in two interpenetrating sublattices α and β. It is useful to define two orthogonal operators that project each state into one of the sublattices,

$$P_\alpha = \sum_{i \in \alpha} |i\rangle\langle i|, \tag{6}$$

$$P_\beta = \sum_{j \in \beta} |j\rangle\langle j|.$$

Therefore, any eigenvector $|\phi\rangle$ of H_{AA} can be written in terms of these projectors:

$$H_{AA}(P_\alpha + P_\beta)|\phi\rangle = E(P_\alpha + P_\beta)|\phi\rangle. \tag{7}$$

Since H_{AA} produces a hopping in the wave-function between the α and β sublattices, it is clear that

$$H_{AA}P_\alpha|\phi\rangle = EP_\beta|\phi\rangle, \tag{8}$$

$$H_{AA}P_\beta|\phi\rangle = EP_\alpha|\phi\rangle. \tag{9}$$

From these equations, one can see that the spectrum is symmetric around $E=0$, since if $(P_\alpha+P_\beta)|\phi\rangle$ is an eigenvector with eigenvalue E, $(P_\alpha-P_\beta)|\phi\rangle$ is also an eigenvector with eigenvalue $-E$.

We can decouple the sublattices by further applying H_{AA} to Eqs. (8) and (9):

$$H_{AA}[H_{AA}(P_i|\phi\rangle)] = H_{AA}^2(P_i|\phi\rangle) = E^2(P_i|\phi\rangle), \tag{10}$$

where $i=\alpha,\ \beta$. Thus, the projection of an eigenvector in each sublattice is a solution of the squared Hamiltonian. Observe that the eigenvalues of H_{AA}^2 are positive definite, and their eigenstates are, at least, doubly degenerate. This spectrum can be regarded as the folding of the original spectrum of H_{AA} around $E=0$, in such a way that the two band edges

of H_{AA}, are mapped into the highest eigenvalue of H_{AA}^2, while the states at the center of the original band are now at the minimum eigenvalue of the squared Hamiltonian (E^2).

When $x<x_c^{(s)}$ all A clusters are finite. Therefore, confinement effects are expected, in particular, the band width of H_{AA}^2 is reduced. This helps to explain the appearance of a gap at the center of the A subband of H_{AA} when $x<x_c^{(s)}$, but it does not predict a pseudogap when $x>x_c^{(s)}$.

B. Properties of the H_{AA}^2 spectrum and band edges

The important property of the renormalized Hamiltonian H_{AA}^2 is that the states near $E=0$ have an antibonding nature (the phase between neighbors is π). Since H_{AA}^2 contains odd rings, we expect that frustration of the wave function can prevent the spectrum from reaching its minimum eigenvalue in a continuous form.[15] Furthermore, since there is a cost in energy due to frustration, wave functions tend to avoid regions of higher frustration, and the states begin to localize in regions of lower frustration.[15] The amount of frustration can be estimated from the numerical results and using statistics. One can show that this frustration augments with disorder. To see this, it is convenient to separate the contribution for each eigenenergy into three parts, one due to the self-energy, and the other two given by the bonds with positive (bonding) and negative (antibonding) contribution to the energy. This separation goes as follows. First we write the equation of motion for H_{AA}^2

$$(E^2-Z_iV^2)c_i(E)=\sum_{j\neq i}(H_{AA}^2)_{ij}c_j(E), \tag{11}$$

where $c_i(E)$ is the amplitude of the wave function at site i for an eigenenergy E. After summing over all sites i and using the normalization condition of the wave function, Eq. (11) becomes

$$E^2=\sum_i Z_iV^2|c_i(E)|^2+\sum_{j\neq i}(H_{AA}^2)_{ij}c_j(E)c_i^*(E) \tag{12}$$

$$\equiv C_1(E^2)-C_2(E^2)+C_3(E^2), \tag{13}$$

where $C_1(E^2)=\Sigma_i Z_iV^2|c_i(E)|^2$ is the contribution of the self-energies, which depends on the local coordination of the sites. $C_2(E^2)=|\Sigma'_{i,j}(H_{AA}^2)_{ij}c_j(E)c_i^*(E)|$, where the prime means that one considers only those bonds whose product $c_j(E)c_i^*(E)$ is negative. This is an antibonding contribution. Finally, $C_3(E^2)$ is similar to $C_2(E^2)$, except that the summation is over bonds with positive $c_j(E)c_i^*(E)$. This equation is valid for all E. At the upper band edge $C_2(E^2)$ is zero because in a perfect bonding state all the site amplitudes have the same sign. The state $E^2=0$ corresponds to a configuration where the sign of the wave amplitude alternates between nearest neighbors, and the bond contribution $[C_3(E^2)-C_2(E^2)]$ is equal to the self-energy. $C_3(E^2)$ is a measure of the contribution of bonds that are frustrated, while $C_3(E^2)-C_2(E^2)$ gives the amount of frustration compared with the antibonding term.

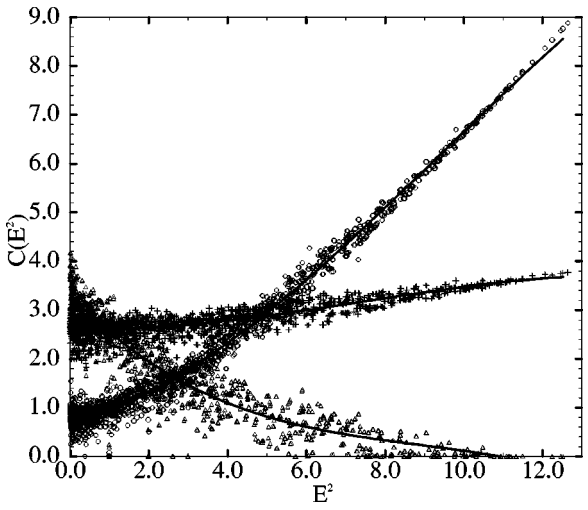

FIG. 3. Contributions to E^2 of $C_2(E^2)$ (circles), $C_3(E^2)$ (triangles), and $C_1(E^2)$ (crosses). These data were obtained from the calculation shown in Fig. 1(a).

These three contributions for the same lattices as in Fig. 1(a) are shown in Fig. 3. Notice that $C_1(E^2)$ (crosses) and $C_3(E^2)$ (circles) decrease towards $E=0$. The contribution $C_2(E^2)$ (triangles) increases from zero at the band edge, to a maximum value near $E=0$, except in some energies where $C_2(E^2)$ is zero. A detailed analysis reveals that each of them is a degenerate state, producing high peaks in the DOS. These states correspond to isolate clusters and produce sharp peaks in the DOS [Fig. 1(b)]. For example, the state at $E=1$ corresponds to a doublet of A sites, surrounded by B atoms.

C. Effects of frustration in the lower band edge

To estimate the effects of frustration on the energy spectrum as a function of the concentration of impurities, we need to determine $C_3(E^2)-C_2(E^2)$. This can be done, if first we find bounds for $C_1(E^2)$. Writing Z_i as an average $\langle Z\rangle$ plus a fluctuation part δZ_i, in the expression for $C_1(E^2)$, one obtains

$$C_1(E^2)=\langle Z\rangle V^2+V^2\sum_{i=1}^{N}\delta Z_i|c_i(E)|^2. \tag{14}$$

The amplitude $c_i^2(E)$ can be written as an average plus a fluctuation $\langle c^2(E)\rangle+\delta c_i^2(E)$ and Eq. (14) becomes

$$C_1(E^2)=\langle Z\rangle V^2+V^2\sum_i \delta Z_i\delta c_i^2(E), \tag{15}$$

where we have used the fact that the sum over all sites of the coordination fluctuations is zero. The last term in Eq. (15) is not zero and corresponds to a correlation between amplitude and coordination fluctuations. We can estimate the corresponding contribution by observing that it is bounded in an statistical sense. It attains a maximum value when in all sites, the sign of the amplitude fluctuation is the same as the fluc-

tuations of the coordination. In a similar way, a minimum is obtained when the fluctuations have opposite signs,

$$-\sum_{i=1}^{N}|\delta Z_i||\delta c_i^2(E)|\leqslant\sum_{i=1}^{N}\delta Z_i\delta c_i^2(E)\leqslant\sum_{i=1}^{N}|\delta Z_i||\delta c_i^2(E)|. \tag{16}$$

The size of the fluctuations in the coordination number is estimated by using the standard deviation of the distribution function of the coordination $[P(Z)]$, which is a binomial distribution (see Appendix A),

$$\sum_{i=1}^{N}|\delta Z_i||\delta c_i^2(E)|\approx\sqrt{4x(1-x)}\sum_{i=1}^{N}|\delta c_i^2(E)|\leqslant\sqrt{4x(1-x)}. \tag{17}$$

Finally, we get the statistical bounds for $C_1(E^2)$

$$V^2[4x-\sqrt{4x(1-x)}]\leqslant C_1(E^2)\leqslant V^2[4x+\sqrt{4x(1-x)}]. \tag{18}$$

This equation can be compared against the results shown in Fig. 3, for $x=0.65$. Equation (18) gives the maximum value of $C_1(E^2)$ as 3.56, in close agreement with 3.58 observed in the upper band edge of Fig. 3. The calculated lower bound is 1.61, in close agreement with the numerical calculations. Notice that these bounds are not strict, due to their statistical nature.

Now, a lower bound for $C_3(E^2)-C_2(E^2)$ can be obtained from the condition $E^2\geqslant 0$. Using this condition, Eqs. (13) and (18) we obtain

$$C_3(E^2)-C_2(E^2)\geqslant -V^2[4x+\sqrt{4x(1-x)}]. \tag{19}$$

From this last result, one can see that the frustration increases with the concentration of impurities. If there is no correlation between fluctuations on amplitude and coordination, the lower bound is $-4x$, but if we allow correlation, a lower energy can be reached by reducing the frustration.

We can also obtain a bound for $C_3(E^2)$ alone. The key idea is to write a new equation, which separates $C_3(E^2)$ from $C_2(E^2)$. This equation is obtained by observing that in the bonding limit (E_+^2), all the bonds are frustrated. From the expected value of the energy calculated for a bonding state, we obtain

$$E_+^2=C_1(E_+^2)+C_3(E_+^2). \tag{20}$$

$C_3(E_+^2)$ can be related with $C_3(0)$ and $C_2(0)$, since if we neglect amplitude variations, the main difference between the bonding and antibonding limit is the sign of the amplitude of the wave function between neighbors. In other words, the total number of bonds must remain constant, and if we change the sign of the contribution from bonds with an antibonding nature in the lowest eigenvalue, we obtain a maximum value for the energy. Amplitude variations can only reduce the frustration, which leads to the inequality

$$C_3(E_+^2)\geqslant C_2(0)+C_3(0). \tag{21}$$

In the perfect square lattice, $C_3(E_+^2)=C_2(0)+C_3(0)$, since each site in H^2 is connected with eight sites: four first neighbors by bonds with hooping integrals $2V^2$ and four second neighbors with hoopings V^2. Thus, when $E=0$, $C_2(0)=8V^2$, and $C_3(0)=4V^2$ since the sign of the wave function alternates between nearest neighbors. In the bonding limit, all the amplitudes have the same sign, and $C_3(E_+^2)=12V^2$. Using Eq. (12) and $C_1(E^2)=4$, one can verify that these values produce the right band edges (0 and 16). As x goes to zero, the difference between $C_3(E_+^2)$ and $C_2(0)+C_3(0)$ grows.

Eliminating $C_2(0)$, using Eq. (13), and the condition that $E^2\geqslant 0$, we obtain

$$C_3(0)\leqslant\frac{E_+^2-C_1(E_+^2)-C_1(0)}{2}=\frac{E_+^2}{2}-4x. \tag{22}$$

E_+^2 is the band width in H_{AA}^2, and can be calculated using the method of fluctuations, as shown in Appendix B. The statistical bound for the frustration is

$$C_3(0)\leqslant 6x^2+2x[\sqrt{3x(1-x)}-1]. \tag{23}$$

D. Estimation of the pseudogap as a function of the concentration of impurities

In the last subsection, we obtained a statistical bound for the frustration $C_3(0)$ at the minimum eigenvalue $E=0$, attained when the correlations in the fluctuations play an important role. To determine the energy where the pseudogap begins (Δ), we need the to determine the frustration $C_3(\Delta^2)$ when these correlations are not allowed in the fluctuations near $E=0$. This could be calculated using a variational procedure similar to the one made for the Penrose tiling.[15] However, due to the statistical nature of this system, such a calculation is extremely difficult. An easier approach takes advantage of the following observation. $C_3(E^2)$ is two times the number of frustrated bonds (since each bond is shared by two sites), and the number of frustrated bonds is proportional to the number of triangles that appear in H_{AA}^2. This number is the third moment of H_{AA}^2 $(\mu_{H_{AA}^2}^3)$ and is proportional to the number of paths with three hops that start and end at the same site. Then, we have for the value of $C_3(E^2)$ near $E=0$,

$$C_3(E^2)=K\mu_{H_{AA}^2}^{(3)}=K\mu_{H_{AA}}^{(6)}, \tag{24}$$

where K is a constant (3 in the perfect square lattice), which depends on the concentration x. But from Sec. II the states at $E=0$ produce a weight at $E=0$ that affects the moments, that can be avoided by defining a renormalized set of moments $\mu^{*(n)}$. In a similar way, we can obtain a renormalized value of $C_3(E^2)$, which does not give weight to the states at $E=0$, and can be associated with the value of the frustration without the fluctuations at a higher energy Δ. Therefore,

$$C_3(\Delta^2)=K\mu_H^{*(6)}=\frac{1}{1-f_0(x)}C_3(0)\approx[1+f_0(x)]C_3(0). \tag{25}$$

In Eq. (12) we can substitute this result,

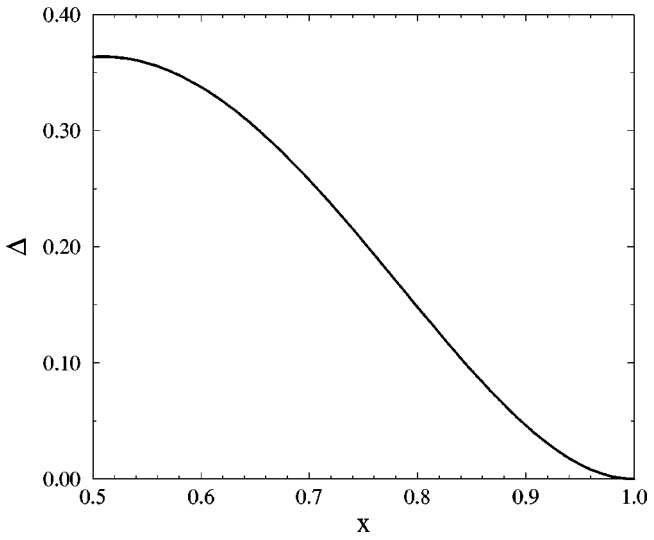

FIG. 4. Bond of the pseudogap Δ in units of V as a function of x, obtained from Eq. (28).

$$\Delta^2 = C_1(\Delta^2) - C_2(\Delta^2) + C_3(\Delta^2) \tag{26}$$

$$\geqslant C_1(0) - C_2(0) + C_3(\Delta^2)$$

$$\approx f_0(x) C_3(0), \tag{27}$$

where it was used the facts that $C_2(0) \geqslant C_2(\Delta^2)$ and $C_1(\Delta^2) \approx C_1(0)$. Finally, using Eq. (23) we obtain

$$\Delta \geqslant \sqrt{f_0(x)\{6x^2 + 2x[\sqrt{3x(1-x)} - 1]\}}. \tag{28}$$

In Fig. 4, we show a plot of this equation, giving $\Delta = 0.3$ for $x = 0.65$. This formula is only valid for $x > x_c$, since for lower x, the quantum confinement plays an important role, and localization does not reduce the energy, because there is a competition between frustration and quantum confinement effects, which in fact turns the pseudogap into a real gap.

An interesting feature that appears in Eq. (28), is the relationship between the pseudogap and the degeneracy. This relation was conjectured long ago,[13] when it was suggested that the central gap in the Penrose lattice was a consequence of the collapse of states into the central peak. However, both effects are due to the frustration of states, because frustration produces degeneracy due to a narrowing of the band width. In this case, the degeneracy is observed in the states at $E = 0$. The approach developed here can be extended to the cubic random binary alloy, where a pseudogap of the DOS and confined states were found at the middle of the spectrum. Another interesting example of a lattice showing this behavior is the Penrose tiling.[15]

IV. CONCLUSIONS

We calculated the first moments of a random binary alloy in a square lattice by using the Cyrot-Lackmann theorem. The results show that there is a transition of the spectrum, from unimodal to bimodal behavior, as a function of the concentration of impurities. This transition occurs near the geometrical percolation threshold. These ideas are made clear by using the bipartite symmetry of the square lattice once the impurity atoms are removed. This lets us focus on only one sublattice, that defines a ''squared'' Hamiltonian that contains odd member rings in the disordered alloy. In this picture, the states near the center of the spectrum are mapped to the lower band edge, and require a large number of nodes, as a sort of antiferromagnetic order, and thus frustration effects are responsible for the depletion of the LDOS near the minimum eigenvalue of H^2. With these techniques we were able to estimate not only the band width of the disordered system but also the size of the pseudogap in the center of the spectrum.

ACKNOWLEDGMENTS

We would like to thank Professor R.J. Elliott for useful discussions. This work was supported by CONACyT through Grants No. 32148-E, and DGAPA UNAM Projects No. IN108199, IN105999, IN101701, and IN104598.

APPENDIX A: THE FIRST MOMENTS OF A RANDOM BINARY ALLOY

For calculating all the required moments in the split-band limit, we need to count all the possible paths that visit A sites that start and return to the same site. One must take into account all possible local configurations of disorder. Thus, Eq. (3) must be considered in a statistical way, by including the probability of a path connecting A sites with n hops. We can define the configurational averaged spectral moments $\langle \mu_i^{(n)} \rangle$ as

$$\langle \mu_i^{(n)} \rangle = \sum_{j_1, \ldots, j_{n-1} \in A} P(i, j_1, \ldots, j_{n-1}) \times H_{ij_1} H_{j_1 j_2} \cdots H_{j_{n-1} i}. \tag{A1}$$

where $P(i, j_1, j_2, \ldots, j_{n-1})$ is the probability of a given path.

All the odd moments are zero because there is no possibility of returning to the starting point with an odd number of steps in the square lattice. If the B sites are forbidden, the clusters of A sites retain this property, while if δ is finite, the odd moments are not zero, and then the subband A is no longer symmetric around $E = 0$.

The second moment is always equal to the local coordination on A sites:

$$\mu_i^{(2)} = Z_i V. \tag{A2}$$

There are only five different local configurations, with coordination 0, 1, 2, 3, and 4, respectively. The probability of each coordination $P(Z)$ around a given site is given by a binomial distribution

$$P(Z) = C_Z^4 x^Z (1-x)^{4-Z}, \tag{A3}$$

where C_Z^4 are the combinations of four in Z. This factor takes care of the different geometrical possibilities in which each

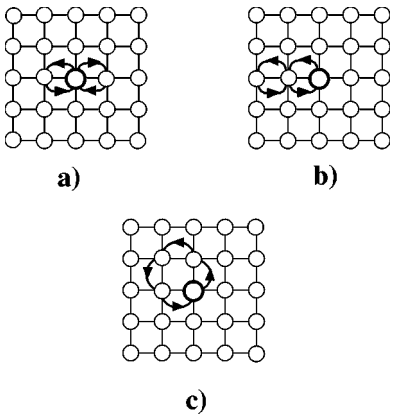

FIG. 5. The three different kinds of paths that contribute to the fourth moment. The central thick circle represents the starting site. The hops are indicated by arrows. (a) The starting site is revisited once. (b) One of the neighbors of the starting site is revisited once. (c) None of the sites are revisited, resulting in a single loop. The presence of *B* atoms reduce the number of loops available.

configuration can occur. The second moment of the DOS corresponds to the sum of the LDOS at all sites. This sum over sites can be written as

$$\langle \mu^2 \rangle = (1/N) \sum_{i=1}^{N} \mu_i^2 = V \sum_{Z=0}^{4} C_Z^4 x^Z (1-x)^{4-Z} Z = 4Vx. \tag{A4}$$

This number gives an estimation of the band width (W), which for the present case is $W = 2\mu^2 = 8Vx$.

The fourth moment calculation requires counting many different configurations and paths. It is convenient to classify the paths as three kinds, as shown in Fig. 5. It is also convenient to calculate paths by grouping the possible clusters according to the coordination of the central site (Z), which is assumed to be of type *A*.

The number of paths of the kind shown in Fig. 5(a) is

$$\langle N_a(Z) \rangle = N_a(Z) = Z^2 \tag{A5}$$

because the condition of revisiting the central site fixes the second and fourth segments of the path. Observe that this quantity does not depend on x, since we are fixing the configuration of the cluster up to first neighbors, and second neighbors are irrelevant for these paths.

The number of paths as in Fig. 5(b) is

$$N_b(Z) = Z \sum_j (Z_j - 1), \tag{A6}$$

since one needs the participation of a second neighbor j to determine if the path is possible or not. Therefore, one has to average over all configurations of a given local coordination we obtain

$$\langle N_b(Z) \rangle = Z \left\langle \sum_j (Z_j - 1) \right\rangle \tag{A7}$$

$$= Z \sum_{l=0}^{3} C_l^3 x^l (1-x)^{3-l} l = 3xZ. \tag{A8}$$

Finally, paths involving four different sites are those shown in Fig.5(c). In principle $\langle N_c(Z) \rangle$ should be proportional to x^2. However, close examination of this situation reveals that only one site closes the loop in all cases. For each coordination number, the average number of paths is given by

$$\langle N_c(1) \rangle = 0, \tag{A9}$$

$$\langle N_c(2) \rangle = 2\frac{2}{3}x, \tag{A10}$$

$$\langle N_c(3) \rangle = 2 \sum_{l=0}^{2} C_l^2 x^l (1-x)^{2-l} l = 4x,$$

$$\langle N_c(4) \rangle = 2 \sum_{l=0}^{4} C_l^4 x^l (1-x)^{4-l} l = 8x,$$

where there are two senses of circulation for each loop. Notice that for $Z=2$, a loop is not possible if the two neighbors are in opposite sites.

Therefore, the fourth moment for a site of coordination Z is

$$\mu_Z^4 = V^2 [Z^2 + 3xZ + \langle N_c(Z) \rangle]. \tag{A11}$$

The corresponding parameter s_Z can be calculated using these results,

$$s_1 = 3x, \quad s_2 = \frac{11}{6}x, \quad s_3 = \frac{13}{9}x, \quad s_4 = \frac{5}{4}x. \tag{A12}$$

Higher coordination has always a lower value of the parameter s_Z. Using the distribution function for each coordination, we can calculate an average $\langle s \rangle$ defined as

$$\langle s \rangle = \sum_{Z=0}^{4} P(Z) s_Z. \tag{A13}$$

APPENDIX B: ESTIMATION OF THE UPPER BAND EDGE (E_+^2)

The bonding limit of the energy spectrum corresponds to a maximum value of E_+^2, attained when $C_3(E^2) - C_2(E^2)$ and $C_1(E^2)$ are maxima. From Eq. (18), the maximum value of $C_1(E^2)$ is $4x + \sqrt{4x(1-x)}$. The maximum value of $C_3(E^2) - C_2(E^2)$ is obtained from observing that if all the amplitudes have the same sign,

$$\sum_{i,j} (H_{AA}^2)_{ij} c_i^*(E) c_j(E) \leqslant \langle (H_{AA}^2)_{ij} \rangle + F, \tag{B1}$$

where F are the fluctuations in the distribution of the squared Hamiltonian.

It is easy to see that $\langle (H_{AA}^2)_{ij} \rangle$ in H_{AA}^2 is exactly the number of $N_b(Z)$ paths that are considered in Appendix A, where their number is calculated for a given coordination number. Using Eq. (A7) and averaging over Z one obtains

$$\langle (H_{AA}^2)_{ij} \rangle = V^2 \langle \langle N_b(Z) \rangle \rangle = 3xV^2 \sum_{Z=0}^{Z=4} P(Z)Z = 12x^2V^2. \tag{B2}$$

The size of the fluctuations is evaluated by an average of the fluctuations in the distribution of $N_b(Z)$ for each coordination number

$$F \approx \sqrt{3x(1-x)}V^2 \sum_{Z=0}^{Z=4} P(Z)Z = 4xV^2\sqrt{3x(1-x)}. \tag{B3}$$

The band edge of H_{AA}^2 is given by the sum of contributions (B2) and (B3)

$$E_+^2 = \pm V^2\{12x^2 + 4x[1+\sqrt{3x(1-x)}] + \sqrt{4x(1-x)}\}. \tag{B4}$$

This method gives a much better estimation for the upper band edge, which is usually approximated[20] by $\langle Z \rangle V$. The square root of E_+^2 gives an estimation of the band edges in H_{AA}. For example, if $x=0.65$ this formula gives $E_+=3.3$. This approximation can be compared with Fig. 1, where the band edge is near 3.4. The usual estimation $4x=2.6$ is not as good as Eq. (B4). Equation (B4) gives a better estimation because it includes information about H_{AA}^2 and the size of the fluctuations, which is related with the size of the exponential Lifshitz tails that appear in the band edges.

[1] N.F. Mott and E.A. Davis, *Electronic Processes in Non-crystalline Materials* (Oxford University Press, Oxford, 1979).

[2] S. Kirkpatrick and T.P Eggarter, Phys. Rev. B **6**, 3598 (1972).

[3] Ziman, *Models of Disorder* (Cambridge University Press, Cambridge, 1979).

[4] C.M Soukoulis, E.N Economou, and G.S Grest, Phys. Rev. B **36**, 8649 (1987).

[5] R. Berkovits and Y. Avishai, Phys. Rev. B , R16 125 (1996).

[6] C.M Soukoulis, Q. Li, and G.S Grest, Phys. Rev. B **45**, 7724 (1992).

[7] E.N Abrahams, P.W Anderson, D.C Licciaredello, and T.V Ramakrishnan, Phys. Rev. Lett. **42**, 673 (1979).

[8] Y. Meir, A. Aharony, and B. Harris, Europhys. Lett. **10**, 275 (1989).

[9] C.M Soukoulis G.S Grest, Phys. Rev. B **44**, 4685 (1991).

[10] G.G. Naumis, R.A. Barrio, and Chumin Wang, in *Proceedings of the 5th International Conference on Quasicrystals*, edited by Ch. Janot and R. Mosseri (World Scientific, Singapore, 1995), p. 514.

[11] R.A. Barrio, G.G. Naumis, and Ch. Wang, in *Current Problems in Condensed Matter*, edited by J.L. Morán López (Plenum Press, New York, 1998), p. 283.

[12] G.G Naumis, J. Phys.: Condens. Matter **11**, 7143 (1999).

[13] M. Kohmoto and B. Sutherland, Phys. Rev. Lett. **56**, 2740 (1986).

[14] M. Arai, T. Tokihiro, T. Fujiwara, and M. Kohmoto, Phys. Rev. B **38**, 1621 (1988).

[15] G.G Naumis, R.A Barrio, and Ch. Wang, Phys. Rev. B **50**, 9834 (1994).

[16] S.J Poon, Adv. Phys. **4**, 303 (1992).

[17] E. Belin, Z. Dankhazi, A. Sadoc, J.M Dubois, and J.M. Calvayrac, Europhys. Lett. **26**, 677 (1994).

[18] C. Kittel, *Introduction to Solid-state Physics*, 7th. ed. (J Wiley, New York, 1996), p. 614.

[19] F. Cyrot-Lackmann, J. Phys. Chem. Solids **29**, 1235 (1968).

[20] A.P. Sutton, *Electronic Structure of Materials* (Clarendon Press, Oxford, 1993), p. 66.

[21] M. Cohen, in *Topological Disorder in Condensed Matter*, edited by F. Yonezawa and T. Ninomiya, Vol. 46 of Springer Series in Solid State Sciences (Springer, New York, 1983), p. 122.